Bull. Mater. Sci., Vol. 35, No. 3, June 2012, pp. 459–469. © Indian Academy of Sciences.

Experimental and quantum chemical studies on corrosion inhibition performance of quinoline derivatives for MS in 1N HCl

B M MISTRY, N S PATEL, S SAHOO and S JAUHARI*
Applied Chemistry Department, S V National Institute of Technology, Surat 395 007, Gujarat, India

MS received 24 June 2011; revised 2 August 2011

Abstract. **The corrosion inhibition effect of two quinoline derivatives, viz. 2-chloro quinoline 3-carbaldehyde (CQC) and (2-chloro-quinoline-3ylmethyl)-*p*-tolyl-amine (CQA) have been investigated against mild steel (MS) in 1N HCl solution using conventional weight loss, potentiodynamic polarization, linear polarization and electrochemical impedance spectroscopy. The losses in weights of MS samples have proved that both CQC and CQA are efficient inhibitors of corrosion. The mixed mode of inhibition was confirmed by electrochemical polarizations. The results of electrochemical impedance spectroscopy have showed changes in the impedance parameters like charge transfer resistance and double-layer capacitance that confirmed strong adsorption of inhibitors on the MS surface. The inhibition action of these compounds was assumed to occur via adsorption on the steel surface through the active centres contained in the molecules. Furthermore, quantum chemical calculations have been performed at B3LYP/6-31G(d,p) level to complement the experimental evidence.**

Keywords. **Quinoline derivatives; acid corrosion inhibitors; MS; electrochemical impedance spectroscopy; Tafel and polarization methods; DFT.**

1. Introduction

The use of corrosion inhibitor is one of the most effective measures for protecting metal surfaces against corrosion in acidic environments. The corrosion of iron and mild steel (MS) is a fundamental academic and industrial concern that has received a considerable amount of attention (Uhlig and Revie 1985). A study of the mechanism of the action of corrosion inhibitors has relevance both from the point of view of the search for new inhibitors and also for their effective use (Trabanelli 1991). Acid solutions are very commonly used for the removal of undesired scales and rust in many industries. To control corrosion, organic inhibitors are used. In recent times, many organic inhibitors are generally used to protect the metal from corrosion by forming a barrier film on the metal surface. Their effectiveness is related to the chemical composition, their molecular structure, and their affinities to get adsorbed on the metal surface. The addition of corrosion inhibitors effectively secures the metal against an acid attack. Inhibitors are used in these processes to control metal dissolution (Schmitt 1984; Emregul and Hayvali 2004; Khaled *et al* 2004; Quraishi and Sharma 2005) and, during the past decade, many organic inhibitors have been studied in different media (Bentiss *et al* 2006; Prabhu *et al* 2007; Tebbji *et al* 2007; Avci 2008). The mechanism of their action can be different, depending on metal, medium and structure of the inhibitor. One possible mechanism is the adsorption of the inhibitor, which blocks the metal surface and thus does not permit the corrosion process to take place. Organic compounds containing electronegative functional groups and π-electrons in conjugated double or triple bonds generally exhibit good inhibitive properties by supplying electrons via π orbitals. Specific interaction between functional groups and metal surface and heteroatoms like N, O and S play an important role in inhibition due to the free electron pairs which they possess. When both of these features combine, increased inhibition can be observed (Trabanelli 1987; Bentiss *et al* 2000; Muralidharan *et al* 2000; Tebbji *et al* 2005; Saliyan and Adhikari 2008; Yan *et al* 2008).

Schiff base compounds are the condensation products of an amine and a ketone/aldehyde. Recent reports show increased attention to these compounds as corrosion inhibitors in especially acidic environments for various metals like steel, aluminum and copper (Shokry *et al* 1998; Li *et al* 1999; Emregul and Atakol 2004; Emregul and Hayvali 2004; Asan *et al* 2006). The greatest advantage of many Schiff base compounds is that they can be conveniently and easily synthesized from relatively cheap material. Some Schiff bases have been reported earlier as corrosion inhibitors for steel. These compounds, in general, are adsorbed on the metal surface blocking the active corrosion sites. A few research reports revealed that the inhibition efficiency of Schiff's bases are much higher than that of corresponding aldehyde and amines, and this may be due to the presence of a >C=N– group in the molecules (Emregul and Atakol 2004; Emregul and

*Author for correspondence (sj.meenu007@gmail.com)

Hayvali 2004). The planarity (π) and lone pairs of electrons present on N atoms are the important structural features that determine the adsorption of these molecules on the metal surface.

Recently, quantum chemical calculations have been performed enormously to complement the experimental evidences (Levine *et al* 1991). Quantum chemical methods and molecular modeling techniques enable the definition of a large number of molecular quantities characterizing the reactivity, shape and binding properties of a complete molecule as well as of molecular fragments and substituents. The recently developed density functional theory (DFT) quantum chemical calculations have been applied widely to compute electronic properties possibly relevant to the inhibition action. Knowing the orientation of the molecule, favourable configurations, atomic charges and steric and electronic effects would be useful for better understanding of the inhibitor performance. It has been stated that the experimental data can be correlated well with quantum chemical parameters such as electron density, ionization potential, total energy, dipole moment, charge density, highest occupied (HOMO) and lowest unoccupied (LUMO) molecular orbital energies and the gap between them (Patel *et al* 2010).

Keeping the above facts in view, in this communication we have introduced two molecules CQC and CQA (figure 1), and investigated their inhibition action on corrosion of MS in 1N HCl at room temperature and compared their protection powers. Corrosion behaviours of MS in 1N HCl media in the absence and presence of both the inhibitors have been studied by weight loss method, potentiodynamic polarization, linear polarization and electrochemical impedance spectroscopy (EIS).

2. Experimental

2.1 *Materials*

MS specimens having compositions of 0·09% P, 0·37% Si, 0·01% Al, 0·05% Mn, 0·19% C, 0·06% S and the remainder Fe were used for the electrochemical polarizations and impedance measurements. The samples of 1×1 cm area were ground with different emery papers of grades 120, 320, 400, 800, 1000 and 2000; they were degreased with AR grade ethanol, acetone and dried at room temperature, and then stored in desiccators before use. The acid solutions were made from analytical grade 37% HCl by diluting with double-distilled water.

2.2 *Preparation of inhibitor compounds*

To a solution of acetanilide (5 mol) in dry DMF (15 mol) at 0–5°C with stirring, $POCl_3$ (60 mol) was added dropwise, and the mixture was stirred at 80–90°C for a period ranging between 4 and 15 h. The mixture was poured into crushed ice and stirred for 5 min. The resulting solid was filtered and washed well with water and dried to give the desired compound, 2-chloro-quinoline-3-carbaldehyde (CQC). The compound was purified by recrystallization from either ethyl acetate or acetonitrile. (IR (KBr, cm^{-1}): 1666, 1581, 1552, 1230, 756; ^{1}H NMR (400 MHz, DMSO-d_6) δ 10·5 (1H, *s*, Ar–CHO), 7·31–8·25 (5H, *m*, Ar-H at quinoline ring) and anal. calcd. for $C_{10}H_6ClNO$: C, 62·68; H, 3·16; N, 7·31%; found: C, 62·71; H, 3·19; N, 7·29%).

The compound CQA was synthesized by stirring the mixture of 2-chloro-quinoline-3-carbaldehyde (CQC)

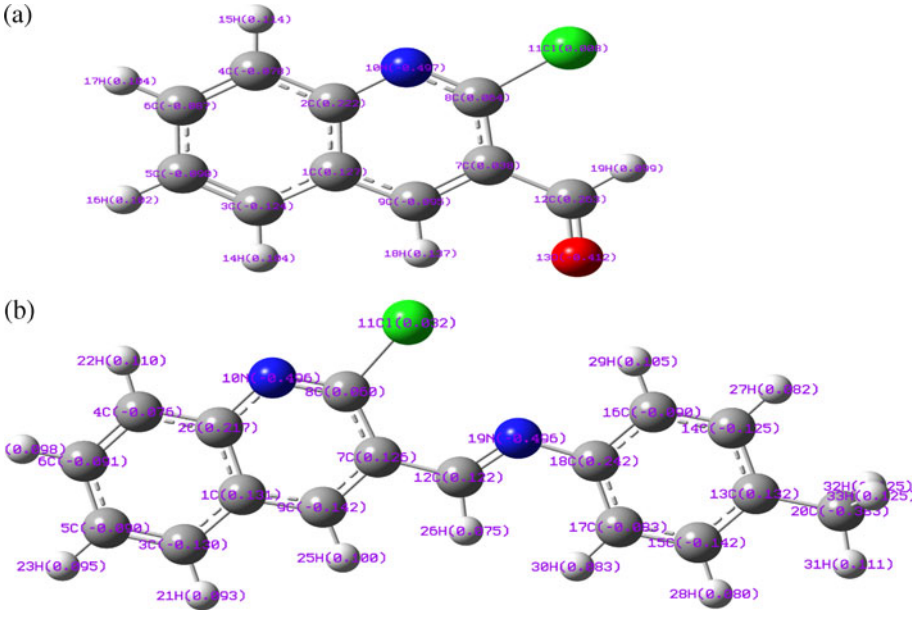

Figure 1. Optimized molecular structure of (**a**) 2-chloro quinoline 3-carbaldehyde (CQC) and (**b**) (2-chloro-quinoline-3-ylmethylene)-*p*-tolyl-amine (CQA) with Muliken's atomic charges obtained at B3LYP/6-31G(*d*,*p*) level.

(0·005 mol) and *p*-methyl aniline (0·005 mol) in ethanol with catalytic amount of sulfuric acid and heated to reflux for 6–7 h. After completion of the reaction (TLC), the reaction mixture was poured onto crushed ice; the solid mass thus separated out was filtered, washed with water and dried to give the desired Schiff base compound (CQA) (Nagaraja *et al* 2006; Chikhlia *et al* 2008). IR (KBr, cm^{-1}): 1664, 1595, 1452, 763; ^{1}H NMR (400 MHz, DMSO-d_6) δ 2·483 (3H, *s*, Ar-C$\underline{H}_3$), 7·209–8·479 (9H, *m*, Ar-H), 8·913 (1H, *s*, –C$\underline{H}$=N–); anal. calcd. for $C_{17}H_{13}ClN_2$: C, 72·73; H, 4·67; N, 9·98%; found: C, 72·70; H, 4·68; N, 9·96%.

2.3 *Scanning electron microscopy*

The surface morphology of the MS specimens immersed in 1N HCl in presence and absence of the CQC and CQA were studied by using scanning electron microscopy. The immersion time of the electrodes for SEM analysis was 12 h. Immediately after the corrosion tests, the samples were subjected to SEM studies to know the surface morphology. SEM Jeol JSM-5610LV was used for the experiments.

2.4 *Weight loss method*

The weight loss measurements were carried out by weighing the prepared specimens before and after immersion for 4 h in 25 ml stagnant test solutions of 1N HCl in the presence and absence of various concentrations of CQC and CQA. From the weight loss data, the percentage inhibition efficiency (IE%) was calculated at different concentrations at 30°C.

2.5 *Potentiodynamic polarization measurements*

All the electrochemical studies were carried out using a three-electrode cell with a platinum counter electrode (CE) and a saturated calomel reference electrode (SCE) and MS sample as the working electrode (WE) using the instrument CH Electrochemical Analyser model 608 C (USA). The electrolytes used were acidic solutions maintained at 30°C. A. C. impedance measurements were shown as Nyquist plots and the polarization data as Tafel plots. Polarization resistance measurements were first carried out with a scan rate of 0·01 V/s at −10 to +410 mV vs corrosion potential (E_{corr}) of the working electrode. The MS electrodes were immersed for 4 h in the test solution for the impedance measurements, which were carried out at E_{corr}.

2.6 *Electrochemical impedance spectroscopy (EIS)*

EIS is now a sophisticated and established laboratory technique, with the relevant software to determine important parameters like charge transfer (corrosion) resistance (R_t) rate and double-layer capacitance (C_{dl}) (Mansfeld 1990; Scully *et al* 1993; Fletcher 1994; Bard and Faulkner 2000; Barsoukov and Macdonald 2005). A.C. impedance measurements were carried out in the range 0·1–1000 Hz. A.C. signal was 5 mV peak-to-peak, with 12 data points per decade. The same cell and system as in the polarization method was used. The double-layer capacitance (C_{dl}) and the charge transfer resistance (R_t) were calculated from Nyquist plots.

2.7 *Computational methods*

The molecular sketches of CQC and CQA were drawn using the GaussView 5·08 visualization program. All the quantum calculations were performed using DFT method at B3LYP/6-31G(d,p) level in gas phase with Gaussian 09W software package (Frisch *et al* 2009). The method, B3LYP/6-31G(d,p), has been widely implemented to study the relationship between corrosion inhibition efficiency of the molecules and their electronic properties (Young 2001). We have examined the calculated properties such as electrostatic potential, total energy, dipole moment, charge density, highest occupied (HOMO) and lowest unoccupied (LUMO) molecular orbital energies and the bandgap to evaluate the corrosion efficiency of CQC and CQA.

3. Results and discussion

3.1 *Weight loss measurements*

The corrosion of MS in 1N HCl in the absence and presence of various concentrations (5–25 ppm) of CQC and CQA were studied by the weight loss experiments. The corrosion rate (W_{corr}) and the values of inhibition efficiency (E_w%) were calculated according to following equation:

$$E_w\% = 100 \times \frac{W_0 - W_{corr}}{W_0}, \quad (1)$$

where W_{corr} and W_0 are the corrosion rates of MS with and without the additives, respectively.

The values of E_w%, W_0 and W_{corr} were obtained from weight loss measurements with the addition of various concentrations of CQC and CQA after 4 h of immersion in 1N HCl solutions. From table 1, it was found that the value of E_w% increases with an increase in the concentration of additives which confirmed that the number of molecules adsorbed increased over the MS surface, blocking the active sites from acid attack and, thereby, protecting the metal from corrosion. At the highest concentration of 25 ppm of each additive studied, the E_w% attained was 80% for CQC and 94% for CQA, which confirmed that both of the additives were very effective as inhibitors.

3.2 *Potentiodynamic (Tafel) polarization measurements*

To evaluate the effect of CQC and CQA on the electrochemical behaviour of MS, cathodic as well as anodic polarization studies were carried out by recording the Tafel plots

Table 1. Inhibition efficiency of MS in 1N HCl in presence and absence of different concentrations of CQC and CQA (weight loss method).

Inhibitor	IC (mg kg^{-1})	W (μg cm^{-2} h^{-1})	E_w%
CQC	1N HCl	18·800	–
	5	12·756	32
	10	08·989	52
	15	06·512	65
	20	04·856	74
	25	03·712	80
CQA	1N HCl	18·800	–
	5	10·855	42
	10	06·708	64
	15	04·123	78
	20	02·389	87
	25	01·098	94

IC, inhibitor concentration.

(figures 2 and 3). The corrosion kinetic parameters such as corrosion potential (E_{corr}), corrosion current density (I_{corr}), anodic and cathodic Tafel slopes (b_a and b_c) were derived from these curves and are given in table 2. The values of inhibition efficiency (E_I%) were calculated using the following equation:

$$E_I\% = 100 \times \frac{I_{corr} - I_{corr(inh)}}{I_{corr}}, \quad (2)$$

where I_{corr} and $I_{corr(inh)}$ represents the values of corrosion current densities without and with the additives, respectively and were determined by extrapolation of the cathodic and anodic Tafel lines to the corrosion potential, E_{corr}. It was found from table 2 that the values of E_I% increased with increase in the concentration of both the additives. At the highest concentration of 25 ppm, the values of E_I% were 94·32% and 98·69% for CQC and CQA, respectively which confirmed the strong adsorption on the MS surface to control the corrosion rates.

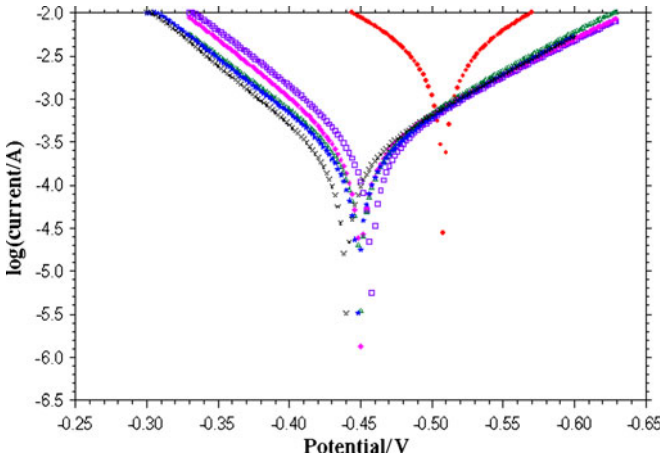

Figure 2. Tafel plots showing effect of CQC on corrosion of MS in a HCl medium (● 1N HCl, ⋇ 25 mg kg^{-1}, ★ 20 mg kg^{-1}, △ 15 mg kg^{-1}, ◆ 10 mg kg^{-1} and □ 5 mg kg^{-1}).

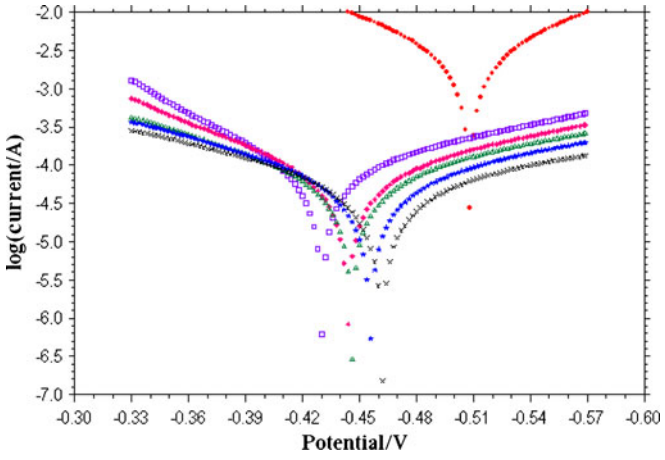

Figure 3. Tafel plots showing effect of CQA on corrosion of MS in a HCl medium (● 1N HCl, ⋇ 25 mg kg^{-1}, ★ 20 mg kg^{-1}, △ 15 mg kg^{-1}, ◆ 10 mg kg^{-1} and □ 5 mg kg^{-1}).

The inhibiting properties of the tested CQC and CQA have also been evaluated by determining the polarization resistance, R_p (Ω cm^2). The corresponding polarization resistance (R_p) values for MS in 1N HCl in the absence and presence of different concentrations of the additives are given in table 2. The values of inhibition efficiency (E_{RP}%) were calculated as follows:

$$E_{RP}\% = 100 \times \frac{R_{p(inh)} - R_p}{R_{p(inh)}}, \quad (3)$$

where R_p and $R_{p(inh)}$ are the polarization resistances in the absence and presence of the additives, respectively.

It was observed that the Tafel plots in 1N HCl solution for MS with different concentrations of CQC and CQA were almost similar (figures 2 and 3). Corrosion currents obtained with the additives were lower than the corrosion current obtained for MS in 1N HCl solution without inhibitors. Both have acted as effective corrosion inhibitors suppressing both anodic and cathodic reactions due to their adsorption on the MS surface, blocking the active sites (Riggs 1973). Moreover, there was an anodic shift in E_{corr} values to show that the compounds might have retarded anodic reaction of the acid corrosion of MS.

The R_p values of MS in 1N HCl in the absence and presence of different concentrations of the tested additives are also given in table 2. From the observed results, it was found that the R_p values gradually increased with increase in the concentration of the additives. The values of inhibition efficiency (E_{RP}%) of CQC and CQA obtained by electrochemical methods were in good agreement with those of E_I%.

3.3 *Electrochemical impedance spectroscopy (EIS)*

Nyquist plots of EIS for MS in 1N HCl containing different concentrations of CQC and CQA are presented in figure 4.

Table 2. Effect of CQC and CQA on MS in 1N HCl media (electrochemical polarization studies).

Inhibitor	IC ($mgkg^{-1}$)	$-E_{corr}$ (V)	k^a (mV per decade)		I_{corr} (mA cm^{-2})	R_p (Ωcm^2)	E_I%	E_{RP}%
			b_a	b_c				
CQC	1N HCl	0·508	145	135	4·0800	7	–	–
	5	0·458	78	106	0·2736	72	93·29	90·27
	10	0·450	80	109	0·2612	77	93·59	90·90
	15	0·450	82	111	0·2542	88	93·76	92·04
	20	0·448	84	113	0·2483	96	93·91	92·70
	25	0·440	86	114	0·2314	106	94·32	93·39
CQA	1N HCl	0·508	145	135	4·0800	7	–	–
	5	0·430	71	182	0·0803	276	98·03	97·46
	10	0·444	98	181	0·0749	369	98·16	98·10
	15	0·446	124	193	0·0718	457	98·24	98·46
	20	0·456	137	191	0·0643	540	98·42	98·70
	25	0·462	155	207	0·0531	725	98·69	99·03

[a]Tafel constant.

The values of inhibition efficiency (E_R%) were calculated by the following equation

$$E_R\% = 100 \times \frac{R_{t(inh)} - R_t}{R_{t(inh)}}, \tag{4}$$

where R_t and $R_{t(inh)}$ are the charge transfer resistances (Ω cm^2) values in the absence and presence of the additives, respectively.

To obtain the values of double-layer capacitance (C_{dl}), the values of frequency at which the maximum imaginary component of the impedance, $-Z_{im(max)}$, were found and were used in the following equation with corresponding R_t values

$$C_{dl} = \frac{1}{2\pi f_{max} R_t}. \tag{5}$$

Nyquist plots in figures 4(a) and (b) contained depressed semi-circles with the centre under the real axis, whose size increased with the increase in concentration of the additive, confirming that the charge transfer processes mainly controlled the corrosion of MS. An isolated Nyquist plot for MS, the blank system, is shown in figure 4(c) and the value of real impedance (Z') was minimum only, 11 Ω cm^2, which indicated that there was least charge transfer resistance (R_t) of the acid corrosion reactions. There was a gradual increase in the diameter of each of the semicircles of the Nyquist plots when the concentrations were raised from 5 to 25 ppm in figures 4(a) and (b). This gradual increase of the diameters corroborated that the R_t values increased up to the highest concentration of 25 ppm and decrease in C_{dl} is due to the gradual replacement of water molecules by the adsorption of the organic molecules at metal–solution interface, leading to a protective film on the metal surface, then decreasing the extent of dissolution reaction (Stoynov *et al* 1990) and, as a result, the acid corrosion rates of MS gradually decreased.

Table 3 presents values of R_t and C_{dl}. There was a gradual decrease in the value of C_{dl} with an increase in the concentration of both CQC and CQA. The double layer between the charged metal surface and the solution is considered as an electrical capacitor. The adsorption of CQC and CQA on the MS electrode leads to a decrease of its electrical capacity because they might have displaced the water molecules and other ions originally adsorbed on the MS surface. The decrease of this capacity with increasing concentrations of CQC and CQA was associated with the formation of a protective layer on the MS electrode surface. The inhibition efficiency, E_I%, was found to increase with an increase in the concentration of CQC and CQA. Decreasing the capacitance, C_{dl}, resulted from the decrease in local dielectric constant due to the increase of electrical double layer thickness. This suggests that the role of inhibitor molecules is preceded by the adsorption at the metal–solution interface. Therefore, CQC and CQA molecules function by adsorption at the metal–solution interface. Another evidence for the effective adsorption of CQC and CQA on the steel surface can be given from the observation that the maximum frequency (f_{max}) of the capacitive loop of the uninhibited solution is decreased with increasing inhibitor concentration. The results obtained from EIS have shown a similar trend to those obtained from electrochemical polarizations and weight loss measurements.

The results suggested that the corrosion rate of MS was significantly decreased due to the adsorption mechanism affecting both the anodic and cathodic processes. The nature of interaction between the MS surface and inhibitor can be established by isotherm, which describe the adsorption behaviour of the inhibitor on a metal surface.

3.4 *Adsorption isotherm*

The surface coverage (θ) at different concentrations of CQC and CQA in 1N HCl solution was calculated from the corrosion rates obtained by weight loss measurements, using the following equation

$$\theta = \frac{W_0 - W}{W_0}, \tag{6}$$

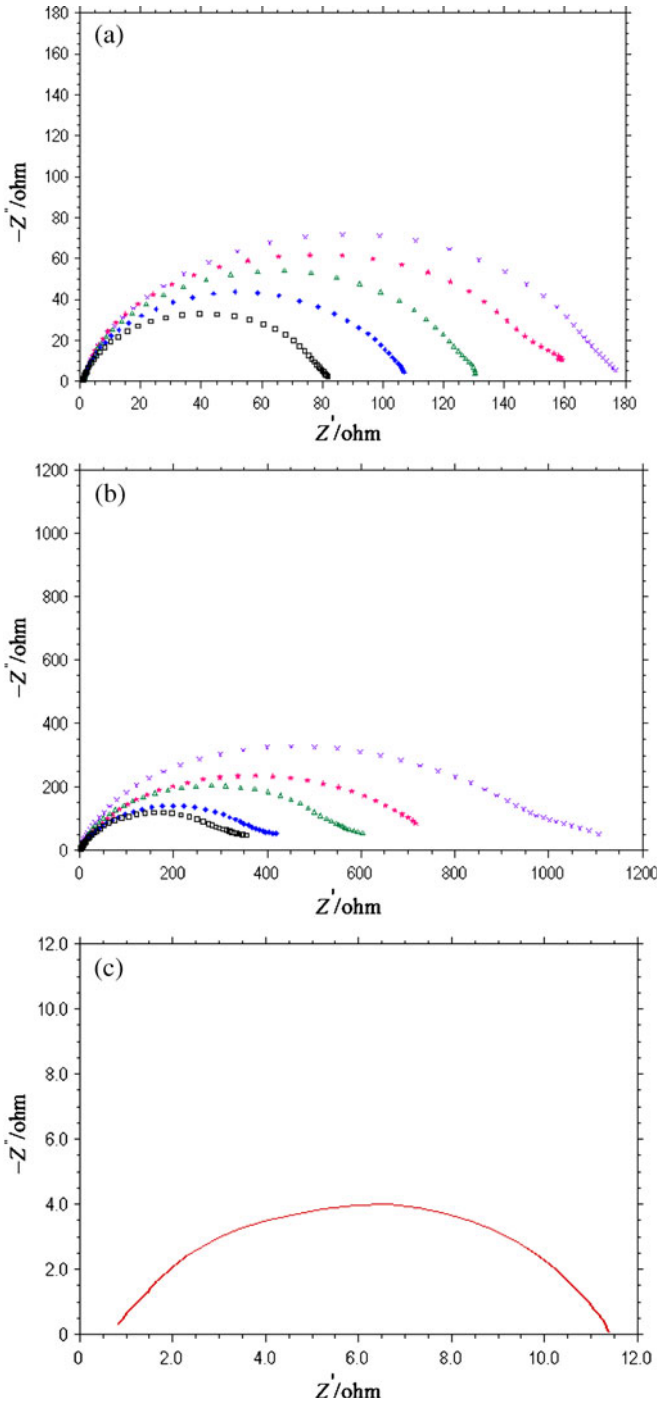

Figure 4. Nyquist plots showing: (**a**) the effect of CQC and (**b**) effect of CQA on corrosion of MS in 1N HCl solution (✕ 25 mg kg^{-1}, ★ 20 mg kg^{-1}, △ 15 mg kg^{-1}, ✱ 10 mg kg^{-1} and □ 5 mg kg^{-1}). (**c**) 1N HCl is a blank system.

where W_0 and W are the corrosion rates in the absence and presence of the inhibitors, respectively.

The adsorption behaviour was described by using the Langmuir isotherm, expressed as:

$$\frac{C}{\theta} = \frac{1}{K_{ads}} + C, \tag{7}$$

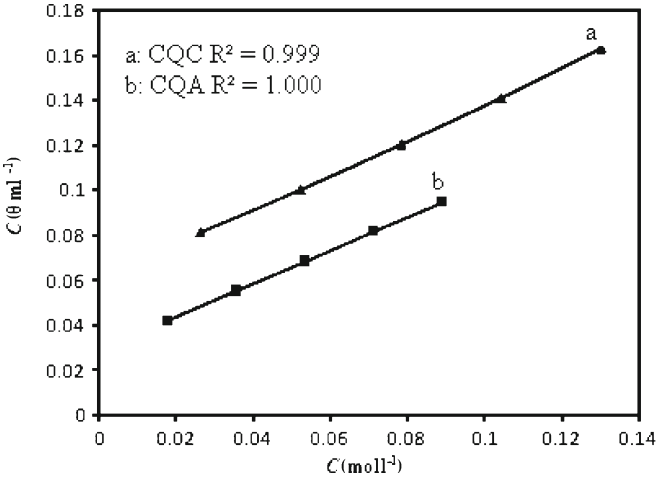

Figure 5. Langmuir isotherm adsorption of CQC and CQA on mild steel in 1 M HCl at room temperature.

Table 3. Data from electrochemical impedance measurements of mild steel in 1N HCl for various concentrations of CQC and CQA.

Inhibitor	IC (mg kg^{-1})	R_t (Ω cm^2)	C_{dl} (μF cm^2)	E (%)
CQC	1N HCl	11	163	–
	5	82	135	86·58
	10	110	121	90·00
	15	132	101	91·66
	20	160	84	93·12
	25	180	74	93·88
CQA	1N HCl	11	163	–
	5	390	109	97·17
	10	480	89	97·70
	15	640	37	98·28
	20	760	25	98·55
	25	1180	12	99·06

where K_{ads} is the equilibrium constant of the inhibitor adsorption process and C the inhibitor concentration. Plots of C/θ vs C yield a straight line, as shown in figure 5. In both cases, the linear regression coefficients (R^2) are almost equal to 1 and the slopes are very close to 1, indicating that the adsorption of CQC and CQA obeys the Langmuir isotherm. Further, the K_{ads} values were calculated from the intercepts of the straight lines on the C/θ-axis. The constant of adsorption (K_{ads}) is related to the standard free energy of adsorption, ΔG^0_{ads}, with the following equation:

$$\Delta G_{ads} = -2{\cdot}303RT \log (55{\cdot}5K_{ads}), \tag{8}$$

where K_{ads} is the equilibrium constant of adsorption, R the gas constant, T the absolute temperature and the value 55·5 is the molar concentration of water solution in mol l^{-1}.

The addition of inhibitors causes negative values of ΔG^0_{ads}, which indicate that the inhibitors CQC and CQA are adsorbed spontaneously. It is generally accepted that, for values of ΔG^0_{ads} up to -20 kJ mol^{-1}, the types of adsorption were termed as physisorption, because the inhibition

acts due to the electrostatic interactions between the charged molecules and the charged metal, while the values around −40 kJ mol^{-1}, were seen as chemisorptions (Donahue and Nobe 1965; Kamis *et al* 1991), which is due to the charge sharing or a transfer from the inhibitor molecules to the metal surface to form a covalent bond. The values of ΔG^0_{ads} in our measurements range from −33·44 kJ mol^{-1} to −34·99 kJ mol^{-1}, which suggests that the adsorption of CQC and CQA involves two types of interaction, viz. chemisorption and physisorption (Mistry *et al* 2010).

3.5 *Quantum chemical study*

Quantum chemical studies have been successfully implemented to correlate the corrosion protection efficiency of organic inhibitors with their calculated molecular orbital (MO) energy levels (Bahrami *et al* 2010; Gece and Bilgic 2010; Ayatia *et al* 2011). To investigate the influence of electronic structure on the corrosion efficiency of the compounds, CQC and CQA, some parameters such as the energies of molecular orbital, E_{HOMO} (highest occupied molecular orbital), E_{LUMO} (lowest unoccupied molecular orbital energy) and the dipole moment (μ) were calculated at B3LYP/6-31G(d,p) level in gas phase. The calculated results are given in table 4. E_{HOMO} often is associated with the electron donating ability of the molecule. High values of E_{HOMO} are likely to indicate a tendency of the molecule to donate electrons to appropriate acceptor molecules to the unoccupied d orbital of a metal. As we know the electronic configuration of Fe atom is [Ar] $4s^2 3d^6$, and $3d$ orbital is not fully filled with electrons. The unfilled $3d$ orbital could bind with HOMO of the inhibitors (Zhao *et al* 2005), whereas the filled $4s$ orbital could donate the electron to LUMO of the inhibitors. So, it can be predicted that the adsorption of inhibitors on the MS surface may be ascribed to the interaction between $3d$, $4s$ orbitals of Fe atom and the front molecular orbitals of the inhibitor (Bentiss *et al* 2004). Whereas, the energy of the lowest unoccupied molecular orbitals indicates the ability of the molecule to accept electrons. The lower the value of E_{LUMO}, the more probability of the molecule to accept electrons. Based on the parameters summarized in table 4, the higher E_{HOMO} and the lower energy bandgap ($\Delta E(\text{eV}) = E_{LUMO} - E_{HOMO}$) of CQA may enhance its corrosion efficiency as compared to CQC (Ju *et al* 2008), that corroborate well with our experimental findings where CQA showed ∼5% more corrosion efficiency than CQC.

Table 4. Quantum chemical parameters of inhibitors obtained using B3LYP/6-31G(d,p) method.

Inhibitors	Total energy (a.u.)	μ (D)	E_{HOMO} (eV)	E_{LUMO} (eV)	E (eV)
CQC	−974·85	3·703	−0·25302	−0·09174	0·16128
CQA	−1225·35	4·339	−0·21851	−0·07744	0·14107

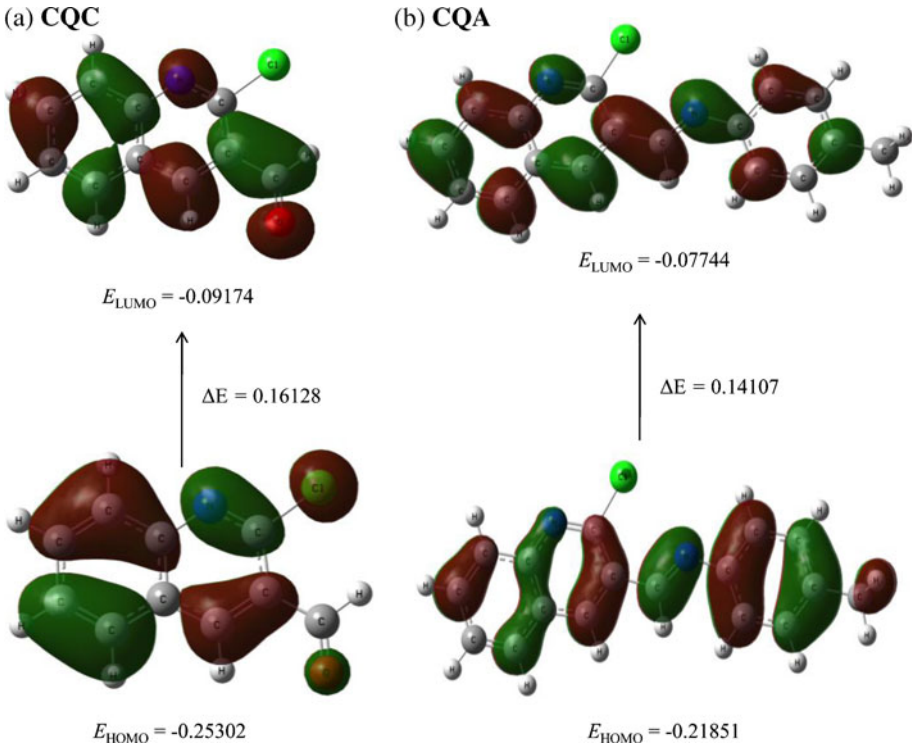

Figure 6. Calculated HOMO and LUMO molecular orbitals of studied molecules using B3LYP/6-31G (d,p) method: (**a**) CQC and (**b**) CQA.

The HOMO and LUMO diagrams (figure 6) of the inhibitors, CQA and CQC, reflect that the orbital electron densities were distributed homogeneously throughout the molecules. Therefore, the Mulliken atomic charges (figure 1) were examined to explain the inhibition approach by the studied molecules. The more negative the atomic charges of the adsorbed inhibitors, the more easily the atom donates its electrons to the unoccupied orbital of the metal and adsorb preferentially on the metal surface with the formation of a closely packed adsorption layer to inhibit iron ions from entering the solution. It is clear from figure 1 that nitrogen atoms carrying negative charges could offer electrons to the metal surface to form a coordinate type bond. CQA with two negatively charged N-donor atoms may prefer adsorption of soft iron ion as compared to CQC with one negatively charged N-donor atom. Furthermore, the MEP spectrum is mapped so that the most negative potential is assigned to be red, the most positive potential is assigned to be blue, and the colour spectrum is mapped to all other values by linear interpolation and has been plotted for the compounds CQC and CQA from the B3LYP/6-31G (d,p) optimized geometry in gas phase (figure 7). The negative regions in MEP can be regarded as nucleophilic centres, whereas regions with positive electrostatic potential are potential electrophilic sites. The quantum chemical studies of CQC and CQA suggest that inhibition efficiency also depends, on the distribution of negative charge. Figure 7 clearly reveals that both the inhibitors contained two nucleophilic centres, but in CQC the negative centres are distributed on the opposite side of the molecule whereas in case of CQA, it is on the same side. This charge distribution in CQA resulted in the improved, corrosion inhibition than CQC due to more access of negative charge to the metal surface.

3.6 *SEM analysis*

In order to evaluate the conditions of MS surfaces in contact with 1N HCl acid solution, a superficial analysis was carried out. Figure 8(a) shows polished MS sample. Figure 8(b) shows SEM images of the surface of the MS specimens after immersion in 1N HCl with no additives for a duration of 12 h. The surface seen in the figure was a result of cracks caused by corrosion due to exposure of MS to 1N HCl. Figures 8(c) and (d) show images of the surface of the MS specimens immersed for the same time interval in 1N HCl acid solution containing 25 ppm CQC and CQA. As can be seen from figures 8(c) and (d), we could conclude that there was much less damage on the surface of MS with CQA compared to CQC. This may be due to strong adsorption of CQA on the mild steel surface in 1N HCl solution. It can be concluded from figure 8(d) that corrosion was strongly inhibited when CQA was present in 1N HCl.

3.7 *Inhibition mechanism*

The mechanism of the action of inhibitors in acid solutions has been studied extensively. It is generally believed that these compounds are adsorbed on the metal surface and prevent further dissolution of metal through blocking of either

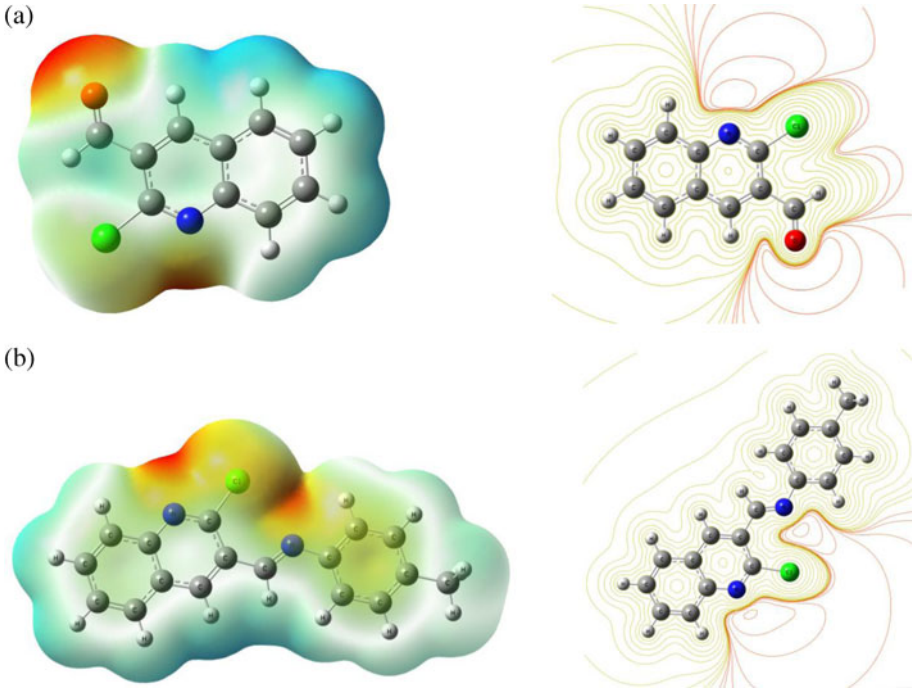

Figure 7. Electrostatic potential map and counter plot of their electrostatic potential of (**a**) CQC and (**b**) CQA, respectively.

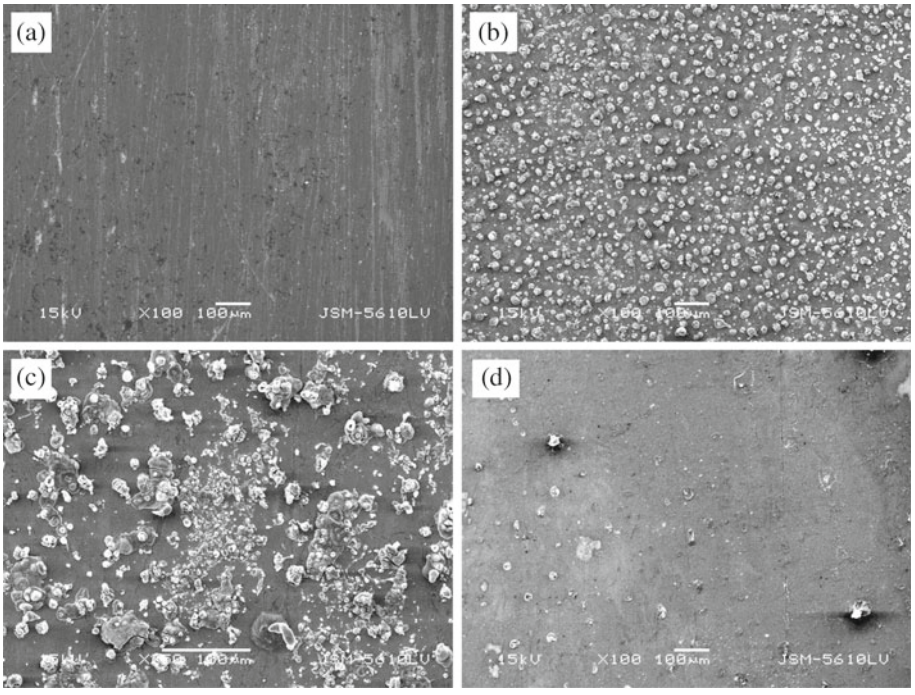

Figure 8. SEM micrographs of MS samples after 12 h immersion period: (**a**) polished surface, (**b**) after 12 h immersion in 1N HCl, (**c**) after 12 h immersion in 1N HCl + 25 ppm CQC and (**d**) after 12 h immersion in 1N HCl + 25 ppm CQA.

the cathodic or anodic reaction or both. Another group of organic inhibitors, which have been the focus of attention in recent years, are those organic compounds capable of forming insoluble complexes, or chelates, with metallic ions present on the surface of metal. The inhibition efficiency of CQC and CQA against the corrosion of MS in 1N HCl can be explained on the basis of the number of adsorption sites, their charge density, molecular size, mode of interaction with the metal surface and the ability to form metallic complex. We can note that a possible mechanism of corrosion inhibition of MS in 1N HCl by the compounds under study may be deduced on the basis of adsorption.

In addition to the chemical adsorption, the inhibitor molecules can also be adsorbed on the steel surface via electrostatic interaction between the charged metal surface and the charged inhibitor molecules if it is possible. The anodic dissolution of iron follows the steps given below (Zhang and Hua 2009):

$$\mathrm{Fe} + \mathrm{Cl}^- \rightleftarrows \left(\mathrm{FeCl}^-\right)_{\mathrm{ads}}, \tag{9}$$

$$\left(\mathrm{FeCl}^-\right)_{\mathrm{ads}} \rightleftarrows \left(\mathrm{FeCl}^+\right)_{\mathrm{ads}} + e^-, \tag{10}$$

$$(\mathrm{FeCl})_{\mathrm{ads}} \rightleftarrows \mathrm{FeCl}^+ + e^-, \tag{11}$$

$$\mathrm{FeCl}^+ \rightleftarrows \mathrm{Fe}^{2+} + \mathrm{Cl}^-. \tag{12}$$

It is well known that the chloride ions have a small degree of hydration and due to specific adsorption, they should be first adsorbed on the positively charged metal surface according to (9). The adsorption of chloride ions creates an excess negative charge towards the solution side of metal and favours more adsorption of cations (Abd El-Makoud *et al* 2003). Then the inhibitor molecules adsorb through electrostatic interactions between the negatively charged metal surface and positively charged molecule (CQC^+ and CQA^+) and form a protective $(\mathrm{FeCl}^-\mathrm{CQC}^+, \mathrm{FeCl}^-\mathrm{CQA}^+)_{\mathrm{ads}}$ layer. In this way, the oxidation reaction of $(\mathrm{FeCl}^-)_{\mathrm{ads}}$ is shown by reaction steps from (10) to (12) (Keles *et al* 2008; Solmaz *et al* 2008a, b).

The cathodic hydrogen evolution reaction may be given as follows

$$\mathrm{Fe} + \mathrm{H}^+ \rightleftarrows \left(\mathrm{FeH}^+\right)_{\mathrm{ads}}, \tag{13}$$

$$\left(\mathrm{FeH}^+\right)_{\mathrm{ads}} + e^- \rightleftarrows (\mathrm{FeH})_{\mathrm{ads}}, \tag{14}$$

$$\left(\mathrm{FeH}^+\right)_{\mathrm{ads}} + \mathrm{H}^+ + e^- \rightleftarrows \mathrm{Fe} + \mathrm{H}_2. \tag{15}$$

Analysis of the electrochemical data showed that the inhibiting properties increased with an increase in the concentrations of CQC and CQA. The inhibition efficiencies increased in the order CQA>CQC at all concentrations. The presence of electron donating groups on the structure increases with the electron density on the N atom, resulting in higher inhibition efficiency. Among the two compounds investigated in the present study, CQA was found to give the best performance as a corrosion inhibitor. This can be explained on the basis of the presence of the –CH=N– group in CQA. Therefore, based on our experimental and theoretical findings, firstly the chloride ions of hydrochloric acid get adsorbed on the metal surface, and in steps led to the formation of ferrous ions. Thereafter, the inhibitors get attracted towards MS and interact coordinatively with ferrous ion,

followed by adsorption on the MS surface to protect the corrosion. The CQA having proper orientation to form chelate with Fe^{+2}, larger electron density distribution on HOMO and lower energy bandgap between HOMO and LUMO resulted in better inhibitory effect than CQC.

4. Conclusions

(I) In this study, it was found that the molecules, CQC and CQA, are effective corrosion inhibitors of MS exposed to 1N HCl solution. CQA was found to be a better corrosion inhibitor than CQC. The inhibition efficiency of the inhibitors increases with an increase in concentration.
(II) The polarization curves inferred that both CQC and CQA are acting as mixed type inhibitors. The results also demonstrate that the inhibition was attributed to the adsorption of the CQC and CQA molecules on the MS surface.
(III) On the other hand, the values of C_{dl} have showed a tendency to decrease, which could be resulting from a decrease in local dielectric constant and/or an increase in thickness of the CQC and CQA through adsorption at the metal/solution interface.
(IV) Weight loss, EIS and polarization techniques gave consistent results from which efficiency of CQC and CQA compounds follow the order: CQA>CQC. Adsorption of CQC and CQA under investigation on MS surface was found to obey the Langmuir adsorption isotherm with standard free energies of adsorption $\left(\Delta G^0_{ads}\right)$ of $-33{\cdot}44$ kJ mol^{-1} and $-34{\cdot}99$ kJ mol^{-1}.
(V) The results of the weight loss, electrochemical polarization and EIS were all in very good agreement to support the above conclusions.
(VI) The calculated quantum chemical properties such as electrostatic potential, charge density, highest occupied (HOMO) and lowest unoccupied (LUMO) molecular orbital energies and the bandgap at B3LYP/6-31G(d,p) level also provide complementary evidences that the molecule, CQA, showed higher corrosion protection efficiency than CQC, which corroborates well with our experimental finding.
(VII) The inhibition efficiencies of the tested inhibitors are highly satisfactory at lower concentrations of 25 ppm and most of the organic inhibitor studied over the years has a history of the concentration ranges much higher than this, and of course higher the concentration, there will be much concern about its environmentally harmful characteristics.

Acknowledgement

The authors thank Director, S V National Institute of Technology, Surat, for providing necessary research facilities.

References

Abd El-Makoud 2003 *Appl. Surf. Sci.* **206** 129
Asan A, Soylu S, Kiyak T, Yildirim F, Oztas SG, Ancin N and Kabasakaloglu M 2006 *Corros. Sci.* **48** 3933
Avci G 2008 *Colloids Surf. A—Physicochem. Eng. Aspects* **317** 730
Ayatia N S, Khandandela S, Momenia M, Moayeda M H, Davoodib A and Rahimizadehc M 2011 *Mater. Chem. Phys.* **126** 873
Bahrami M J, Hosseini S M A and Pilvar P 2010 *Corros. Sci.* **52** 2793
Bard A J and Faulkner L R 2000 *Electrochemical methods: fundamentals and applications* (NY: Wiley Interscience Publications)
Barsoukov E and MacDonald J R 2005 *Impedance spectroscopy: theory, experiment and applications* (NJ: Wiley Interscience Publications) 2nd ed.
Bentiss F, Traisnel M and Lagrenée M 2000 *Corros. Sci.* **42** 127
Bentiss F, Traisnel M, Vezin H, Hildebrand H F and Lagrenee M 2004 *Corros. Sci.* **46** 2781
Bentiss F, Gassama F, Barbry D, Gengembre L, Vezin H, Lagrenee M and Traisnel M 2006 *Appl. Surf. Sci.* **252** 2684
Chikhlia K H, Patel M J and Vashi D B 2008 *ARKIVOC* **13** 189
Donahue F M and Nobe K 1965 *J. Electrochem. Soc.* **112** 886
Emregul K C and Atakol O 2004 *Mater. Chem. Phys.* **83** 373
Emregul K C and Hayvali M 2004 *Mater. Chem. Phys.* **83** 209
Fletcher S 1994 *J. Electrochem. Soc.* **141** 1823
Frisch M J *et al* 2009 *Gaussian 09* (Wallingford, CT: Gaussian Inc)
Gece G and Bilgic S 2010 *Corros. Sci.* **52** 3435
Ju H, Kai Z and Li Y 2008 *Corros. Sci.* **50** 865
Kamis E, Bellucci F, Latanision R M and El-r E S H 1991 *Corrosion* **47** 677
Keles H, Keles M, Dehri I and Serindag O 2008 *Mater. Chem. Phys.* **112** 173
Khaled K F, Babic-Samardzija K and Hacker-man N 2004 *J. Appl. Electrochem.* **34** 697
Levine I N 1991 *Quantum chemistry* (New Jersey: Prentice Hall)
Li S, Chen S, Lei S, Ma H, Yu R and Liu D 1999 *Corros. Sci.* **41** 1271
Mansfeld F 1990 *Electrochim. Acta* **35** 1533
Mistry B M, Patel N S, Patel N J and Jauhari S 2011 *Res. Chem. Intermed.* **37** 659
Muralidharan S, Charasekar R and Iyer S V K 2000 *Proc. Indian Acad. Sci. Chem. Sci.* **112** 127
Nagaraja G K, Prakash G K, Kumaraswamy M N, Vaidya V P and Mahadevan K M 2006 *ARKIVOC* **15** 160
Patel N S, Jauhari S and Mehta G N 2010 *Acta Chim. Slov.* **57** 297
Prabhu R A, Shanbhag A V and Venkatesha T V 2007 *J. Appl. Electrochem.* **37** 491
Quraishi M and Sharma H 2005 *J. Appl. Electrochem.* **35** 33
Riggs Jr. O L 1973 *Corrosion inhibitors* (ed.) C C Nathan (USA: NACE) p. 7
Saliyan V R and Adhikari A V 2008 *Bull. Mater. Sci.* **31** 699
Schmitt G 1984 *Br. Corros. J.* **19** 165
Scully J R, Silverman D C and Kendig M W (eds) 1993 *Electrochemical impedance: analysis and interpretation* (West Conshohocken, PA: ASTM)
Shokry H, Yuasa M, Sekine I, Issa R M, El-Baradie H Y and Gomma G K 1998 *Corros. Sci.* **40** 2173
Solmaz R, Kardas G, Yazici B and Erbil M 2008 *Colloid Surf.* **A312** 7
Solmaz R, Kardas G, Culha M, Yazici B and Erbil M 2008 *Electrochim. Acta* **53** 5941
Stoynov Z and Savova-Stoynova B 1990 *Commun. Dep. Chem. Bulg. Acad. Sci.* **23** 279
Tebbji K, Hammouti B, Oudda H, Ramdani A and Benkadour M 2005 *Appl. Surf. Sci.* **252** 1378

Tebbji K, Bouabdellah I, Aouniti A, Hammouti B, Oudda H, Benkaddour M and Ramdani A 2007 *Mater. Lett.* **61** 799

Trabanelli G 1987 *Chemical industries: corrosion mechanism* (ed.) F Mansfeld (New York: Marcel Dekker) p. 120

Trabanelli G 1991 *Corrosion* **47** 410

Uhlig H H and Revie R W 1985 *Corrosion and corrosion control* (New York: Wiley)

Yan Y, Li W, Cai L and Hou B 2008 *Electrochim. Acta* **53** 5953

Young D C 2001 *A practical guide for applying techniques to real-world problems in computational chemistry* (New York: John Wiley & Sons Inc.) p. 630

Zhang Q B and Hua Y X 2009 *Electrochim. Acta* **54** 1881

Zhao P, Li Y and Liang Q 2005 *Appl. Surf. Sci.* **252** 1596